

Proceedings

Systematic Model-Based Steady State and Dynamic Optimization of Combined Cooling and Antisolvent Multistage Continuous Crystallization Processes [†]

Jiaxu Liu and Brahim Benyahia *

Department of Chemical Engineering, Loughborough University, Loughborough LE11 3TU, UK; j.liu@lboro.ac.uk

* Correspondence: b.benyahia@lboro.ac.uk

† Presented at the 2nd International Electronic Conference on Crystals, 10–20 November 2020; Available online: https://iocc_2020.sciforum.net/.

Published: 31 December 2020

Abstract: Currently, one of the key challenges in the pharmaceutical industry is the transformation of traditional batch production methods into robust continuous processes with the intention of reducing manufacturing costs and time and improving product quality. Crystallization is by far the most important purification technology in Pharma, as more than 80% of the active pharmaceutical ingredients (API) require at least one crystallization step. A successful crystallization process requires tight control over crystal size, shape and polymorphic purity. A rigorous and systematic methodology is presented to design and optimize multistage combined cooling and antisolvent continuous (mixed-suspension, mixed-product removal- MSM-PR) crystallizers. The crystallization of acetylsalicylic acid (API) in ethanol (solvent) and water (anti-solvent) is used as a case study. A predictable and validated mathematical model of the system, which consists of a one-dimensional population balance model, was used to develop several optimizations strategies. Firstly, the attainable region of the mean particle size was determined for both minimum and maximum attainable crystal size. The method helped identify the most suitable number of stages and total residence time or volume for a cascade of continuous crystallizers. This was followed by a steady state optimization which helped determine the optimal operating temperatures and antisolvent flowrates. To minimize the startup time, a series of dynamic optimization strategies were implemented, assuming starting from empty vessels. The optimal dynamic profiles of the temperature and antisolvent flow rate, at different crystallization steps, were identified using a systematic and rigorous approach allowing a reduction in the startup time by 31%.

Keywords: multistage continuous crystallization; cooling and antisolvent crystallization; dynamic optimization; startup and shut down

1. Introduction

Continuous manufacturing is increasingly seen as the most flexible and viable option for the pharmaceutical industry [1]. However, despite the strides forward, many technical challenges are still to be overcome. Continuous pharmaceutical campaigns are anticipated to have short operating windows [2]. This makes the impact of startup and shut down extremely important in both cost of production and environmental impact. To address some of these key issues, the next-generation pharmaceutical plants require systematic, rigorous and robust optimal strategies for process design, operation, and control for single processes and integrated plants [2].

Crystallization is widely used in the pharmaceutical industry for its outstanding efficiency and economic performance in purifying active pharmaceutical ingredients (API). The quality of the final product is commonly determined by the crystal size distribution, shape, and purity, which impact

the downstream processability and drug safety and efficacy. Commonly, the higher average crystal size and lower coefficient of variation (CV) mean higher quality in the pharmaceutical industry [3].

The fundamental driving force for crystallization is supersaturation. Typically, the supersaturation is generated by cooling, solvent evaporation, or the addition of an antisolvent. Most of the crystallization literature is focused on the design, optimization, and control of batch processes. Various model-based and model-free techniques have been extensively implemented and thoroughly discussed in the literature. However only a few decision and control variables are available to optimally design and operate a batch crystallization process. The most common approach is to use the temperature or/and antisolvent ratio to optimize the crystal size distribution, CV, and batch time [4].

Over the last decade, continuous crystallization of API has received a growing interest. To date, most of the literature has focused on three main continuous crystallizers: mixed suspension mixed product removal (MSMPR), plug flow crystallizers and continuous oscillatory baffled crystallizers. Currently, the most dominant type of crystallizer in the pharmaceutical industry is based on a stirred tank design which exploits well-established theory and know-how built over decades of batch crystallization. Consequently, many experimental and modelling efforts have been devoted to continuous MSMPR crystallizers. Several studies focused on the optimization of single, multistage MSMPR and integrated end-to-end continuous pharmaceutical plants with a series of MSMPR crystallizers [1,5,6,7]. Despite the importance of the startup and its anticipated impact on cost and environmental footprint, only a few investigations are reported in the literature, which identified mainly the optimal dynamic profile of the cooling temperature and antisolvent flowrate [8]. However, the MSMPR vessels were assumed to be prefilled with a solution with the steady state composition. This approach is unrealistic and disregards the impact of filling the vessels during the startup, which may extend the startup time even further. To date, only Benyahia and coworkers showed the potential impact of different startup scenarios, including starting from empty MSMPR vessels, on continuous pharmaceutical campaigns [2]. The latter laid the ground for the current investigation, which consists of a systematic optimization approach starting from steady state optimization, aimed at the identification of the attainable mean particle size, followed by different startup optimization strategies including startup from empty vessels.

2. Materials and Methods

The combined cooling and antisolvent crystallization of aspirin (acetylsalicylic acid, ASA) in ethanol (solvent) and water (antisolvent) was considered as a case study. A dynamic mathematical model of the continuous crystallization process (MSMPR) was derived in conjunction with the literature [8], based on several key assumptions summarized below:

- All vessels are assumed to be well-mixed.
- The total volume of the solvent and antisolvent is additive.
- The secondary nucleation, breakage and agglomeration are negligible.

The population balance equations (PBE) of the first and *ith* stages can be written as follows:

$$\frac{\partial V_i n_i(L, t)}{\partial t} = \text{Feed } n_{\text{feed}}(L, t) - F_{\text{out},i} n_i(L, t) - \frac{\partial V_i G_i n_i(L, t)}{\partial L} \quad i = 1 \quad (1)$$

$$\frac{\partial V_i n_i(L, t)}{\partial t} = F_{\text{out},i-1} n_{i-1}(L, t) - F_{\text{out},i} n_i(L, t) - \frac{\partial V_i G_i n_i(L, t)}{\partial L} \quad i = 2, \dots, N \quad (2)$$

where V_i refers to the volume of *ith* stage vessel, feed is the inlet flow rate to the first crystallizer, $n_{\text{feed}}(L, t)$ is the number density function of the crystals in the feed solution, $F_{\text{out},i}$ is the outlet flow rate of *ith* crystallization stage, and G_i is the growth rate of API crystals.

By using the standard method of moment, the *jth* moment at the *ith* stage is defined by:

$$\mu_{j,i}(t) = \int_0^{\infty} L^j n_i(L, t) dL, \quad j = 0, 1, \dots, \infty \quad (3)$$

Assuming that the growth rate G_i is size-independent and the volume V_i is constant. Equations (1) and (2) yield:

$$V_i \frac{d\mu_{j,i}}{dx} = F_{out,i-1}\mu_{j,i-1} - F_{out,i}\mu_{j,i} + V_i G_i j \mu_{j-1,i}, \quad j \geq 1 \quad (4)$$

$$\frac{d\mu_{j,i}}{dx} = \frac{F_{out,i-1}}{V_i} \mu_{j,i-1} - \frac{F_{out,i}}{V_i} \mu_{j,i} + G_i j \mu_{j-1,i}, \quad j \geq 1 \quad (5)$$

In this case study, the growth rate and nucleation rate kinetics, G and B respectively, are adopted from the literature [9] with the kinetic parameters outlined in Table 1.

$$G = k_{G1} \exp\left(-\frac{k_{G2}}{RT}\right) (c^*(S-1))^{k_{G3}} \quad (6)$$

$$B = k_{B1} \exp\left(-\frac{k_{B2}}{RT}\right) \exp\left(-\frac{k_{B3}}{\ln^2 S}\right) \quad (7)$$

Table 1. k_{Gi} and k_{Bi} are empirical parameters.

	k_G	k_B
1	$(3.21 \pm 0.18) \times 10^{-4} \text{ ms}^{-1}$	$(1.15 \pm 0.51) \times 10^{21} \text{ m}^{-3} \text{ s}^{-1}$
2	$(2.58 \pm 0.14) \times 10^4 \text{ Jmol}^{-1}$	$(7.67 \pm 0.11) \times 10^4 \text{ Jmol}^{-1}$
3	1.00 ± 0.01	0.16 ± 0.01

The supersaturation (S) is defined by Equation (8), where c is the concentration of the API at a given time expressed as mass ratio (Equation (9)) and c^* is the concentration at saturation calculated by a polynomial model adopted from the literature [10], and the coefficients are shown in Table 2.

Table 2. Coefficients of the solubility polynomial equation

P_{ij}	1	2	3	4	5	6
1	39.9	4.851	-0.1704	0.007273	-0.0001213	5.949×10^{-7}
2	3.714	0.2022	-0.01658	7.666×10^{-5}	1.14×10^{-6}	
3	0.1693	-0.003634	0.0003186	-3.706×10^{-6}		

The solubility curve of the API (acetylsalicylic acid) is described by a polynomial equation:

$$c^* = P_{11} + P_{21} \times W + P_{12} \times T + P_{31} \times W^2 + P_{22} \times WT + P_{13} \times T^2 + P_{41} \times W^3 + P_{32} \times W^2T + P_{23} \times WT^2 + P_{51} \times W^4 + P_{42} \times W^3T + P_{33} \times W^2T^2 + P_{61} \times W^5 + P_{52} \times W^4T + P_{43} \times W^3T^2 \quad (8)$$

$$S = \frac{c}{c^*} \quad (9)$$

$$c = \frac{M_{API}}{M_{solvent} + M_{antisolvent}} \quad (10)$$

The mass balance of API, solvent and antisolvent are shown in Equations (11)–(16), where ρ_{feed} is the density of feed, ρ_i is the density of the solution density at the i th stage, ρ_c is the density of the crystal, which is 1400 g/kg, and k_v is the shape factor ($\pi/6$).

$$\frac{dM_{API,i}}{dt} = Feed \rho_{feed} (\omega_{s,feed} + \omega_{as,feed}) c_{Feed} - F_{out,1} \rho_1 (\omega_{s,1} + \omega_{as,1}) c_1 - 3\rho_c k_v G_1 \mu_{2,1} V_1, \quad i = 1 \quad (11)$$

$$\frac{dM_{API,i}}{dt} = F_{out,i-1} \rho_{i-1} (\omega_{s,i-1} + \omega_{as,i-1}) c_{i-1} - F_{out,i} \rho_i (\omega_{s,i} + \omega_{as,i}) c_i - 3\rho_c k_v G_i \mu_{2,i} V_i, \quad i = 2, 3 \dots \quad (12)$$

$$\frac{dM_{s,i}}{dt} = Feed \rho_{feed} \omega_{s,feed} - F_{out,i} \rho_i \omega_{s,i}, \quad i = 1 \quad (13)$$

$$\frac{dM_{s,i}}{dt} = F_{out,i-1} \rho_{i-1} \omega_{s,i-1} - F_{out,i} \rho_i \omega_{s,i}, \quad i = 2, 3 \quad (14)$$

$$\frac{dM_{as,i}}{dt} = Feed\rho_{feed}\omega_{as,feed} - F_{out,i}\rho_i\omega_{as,i} + F_{as,i}\rho_{as}, \quad i = 1 \quad (15)$$

$$\frac{dM_{as,i}}{dt} = F_{out,i-1}\rho_{i-1}\omega_{as,i-1} - F_{out,i}\rho_i\omega_{as,i} + F_{as,i}\rho_{as}, \quad i = 2,3 \quad (16)$$

3. Results and Discussion

3.1. Steady State Optimization

The objective of the steady state optimization is to generate the optimal temperature (T_i), antisolvent flow rate ($F_{as,i}$) and residence time (R_i) at each stage, which maximize the average crystal size (L_n). A three-stage continuous crystallization platform is considered where the supersaturation is created by the combination of cooling and antisolvent addition (Figure 1)

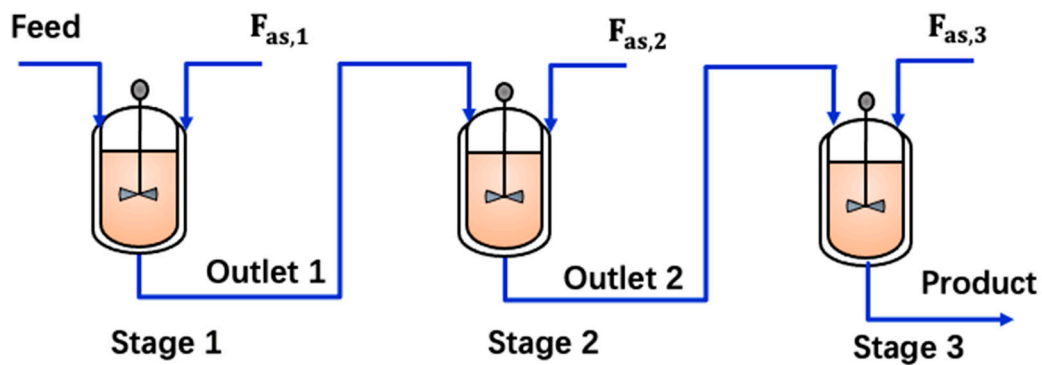


Figure 1. Cascade of three MSMPR crystallizers.

The feed temperature is 40 °C and the minimum and final temperature are both set at 25 °C to generate enough supersaturation. This is captured by the constraints C1 and C7. The concentration of antisolvent is subject to an upper bound which depends on the solubility performance. For the current system, ASA in ethanol (solvent) and water (antisolvent), the solubility of the API decreases as the antisolvent (water) weight ratio increases from 25% to 70%. The maximum antisolvent flow rate in each stage is set at 18.25 g/min, as expressed by the constraint C5. Similarly, the total residence time should not exceed 30 min, while the minimum residence time in each stage is not less than 1 min (constraints C2 and C6). In addition, the constraint C4 ensures that the temperature in the ($i + 1$)th stage is always lower or equal to the temperature of the i th stage, which prevents undersaturated conditions and helps avoid heating which may lead to the dissolving the API crystals.

The mathematical formulation of the steady state single objective optimization problem discussed above is described below:

$$\mathbf{Max}_{T^i, R^i, F_{as}^i} d = \frac{\mu_{1,3}}{\mu_{0,3}} \quad i = 1,2,3$$

s. t. Model equations 5 – 16

$$\mathbf{C1}: 25 \leq T_i \leq 40$$

$$\mathbf{C2}: 1 \leq R_i \leq 30$$

$$\mathbf{C3}: 0 \leq F_{as,i} \leq 18.5$$

$$\mathbf{C4}: T_i \leq T_{i-1}$$

$$C5: \sum_{i=1}^3 F_{as,i} = 18.25$$

$$C6: \sum_{i=1}^3 R_i = 30$$

$$C7: T_3 = 25$$

where $T_i, R_i, F_{as,i}$ are the temperature, residence time and antisolvent flow rate of the i th stage, respectively.

This optimization problem was solved by a genetic algorithm using MATLAB with a population size of 50 and maximum number of generations of 500. The maximum average crystal size obtained was 392 μm , which corresponds to the optimal temperatures, antisolvent flowrates, and residence times outlined in Table 3. The performance of the genetic algorithm can be evaluated by using the difference between the best solution and the mean value in one generation, as shown in Figure 2a. This approach also provides a convergence (stop) criterion for the genetic algorithm.

Table 3. Optimal temperatures, antisolvent flowrates, and residence times obtained in the case of the maximization of the average crystal size.

	Stage 1	Stage 2	Stage 3
Temperature ($^{\circ}\text{C}$)	25.11	25.09	25.00
Antisolvent flow rate (g/min)	2.05	7.59	8.61
Residence time (min)	3.77	10.20	16.03

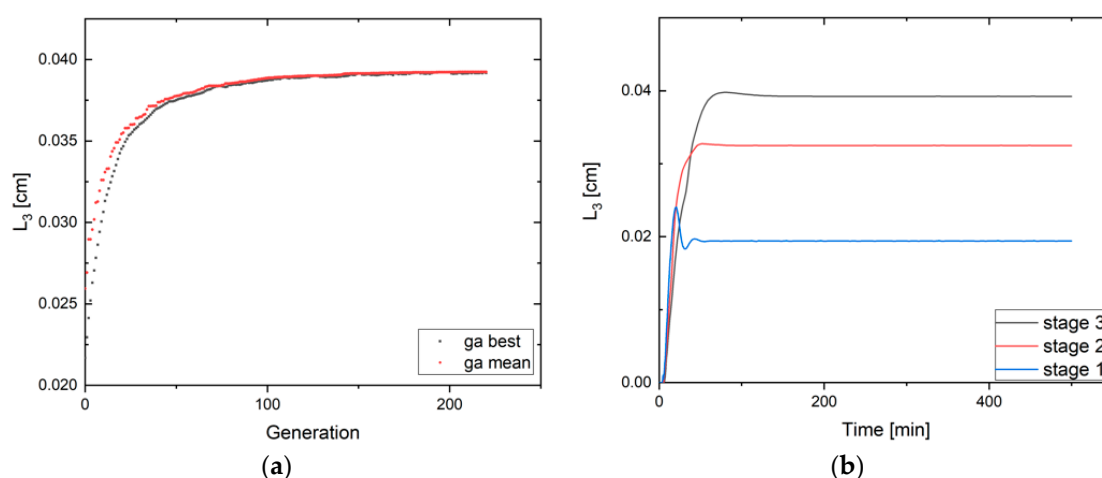


Figure 2. (a) Performance of the genetic algorithm showing the mean and best results of the objective function at different generations. (b) Optimal mean crystal size at different MSMPR stages.

As shown in Figure 2.b, the dynamic profiles of the mean crystal size at different crystallization stages shows that the crystal size nearly doubled at the last stage compared to the first stage, due the high supersaturation generated in stages 2 and 3. The first crystallizer has a short residence time and was dominated by nucleation, making this stage ideal for seed generation, despite some growth exhibited during this stage. Although the dynamic mathematical model was used for the sake of steady state optimization, the results also show the intrinsic startup dynamics during which the crystals produced are off-specification and will be considered as waste. This wasted material represents a significant loss, particularly when considering a short-operation steady state window as anticipated in the pharmaceutical industry [6,11].

3.2. Startup Optimization

As discussed earlier, operating at the steady state optimal conditions (i.e., optimal temperatures and antisolvent flow rates) will ensure the attainment of the maximum mean crystal size at steady state. However, this approach provides no means of control over the intrinsic dynamics exhibited during the startup period during which large amounts of off-specification (waste) material is produced. To minimize the startup time and maximize productivity and reduce wastes, a dynamic optimization approach was developed as described in this section. To allow the dynamic optimization of a process, it is common to optimize piecewise constant and piecewise continuous profiles of the control variables. The approach has been widely used in polymer engineering and related research and industrial sectors [12]. However, only a few startup optimization approaches have been applied to the continuous crystallization processes, as reported in the literature [8]. The reported work focused mainly on one or two crystallization stages and considered the crystallizers as being entirely prefilled. Here, a more systematic and rigorous approach was developed to optimize the startup time of a three-stage MSMPR using piecewise constant profiles of antisolvent flowrate and piecewise continuous profiles of temperatures. The approach also addresses the startup optimization with initially empty vessels. For the sake of brevity, only the optimization results associated with the antisolvent flowrates at different stages are presented here.

The dynamic optimization aims at minimizing the t_{95} , which represents the time to reach the steady state mean crystal size (obtained from steady state optimization) within a relative error band of $\pm 5\%$. The mathematical formulation of the optimization problem is described below.

$$\begin{aligned} & \underset{F_{as,i,k}}{\text{Min}} t_{95}, i = 1, 2, 3, k = 1, 2, \dots, 5 \\ \text{s. t. } & \text{C1: } 0 \leq F_{as,1,k} \leq 4, k = 1, 2, \dots, 5 \\ & \text{C2: } 0 \leq F_{as,2,k} \leq 15.2, k = 1, 2, \dots, 5 \\ & \text{C3: } 0 \leq F_{as,3,k} \leq 20, k = 1, 2, \dots, 5 \end{aligned}$$

Model equations 5 – 16

The piecewise constant (discrete) profile of the antisolvent flowrate consists of five equal time intervals of 10 min. Only the results associated with the antisolvent flow rate, used as decision variables for the startup optimization, are presented here. The three vessels were all kept empty at the beginning. For each stage, the flow rate of antisolvent depends on the feed and the outlet flow rates.

In the optimization problem above, $F_{as,i,k}$ is the antisolvent flow rate of i th stage and k th time intervals. The antisolvent flowrate upper and lower bounds were set in C1–3. The optimization problem was solved using a genetic algorithm in MATLAB. The population and other settings are set the same as for the steady state optimization. The results are summarized in Table 4 below.

Table 4. Optimal antisolvent flow rate profiles obtained by the dynamic optimization approach.

	$F_{as,1}(\text{g/min})$	$F_{as,2}(\text{g/min})$	$F_{as,3}(\text{g/min})$
0–10 min	0.03	1.52	16.47
10–20 min	0.20	9.48	13.06
20–30 min	0.39	5.62	19.80
30–40 min	0.14	9.85	19.88
40–50 min	0.25	9.62	19.32
50–end (steady state setting)	2.05	7.59	8.61

The optimal dynamic profiles of the average crystal size at different stages are shown in Figure 3. With the optimized antisolvent profile, the startup time is shortened to 63.43 min. Compared to the unoptimized startup (startup time of 86.62 min), the optimization saved 23.2 min (26.77% performance improvement) based on a startup from empty vessels and using equally spaced piecewise antisolvent flowrate profiles. When the time interval number is increased to 10, the performance

becomes even better. The startup time is shortened to 61.09 min (31.3% performance improvement). t_{95} was used as an example of the objective function. However, more tight quality requirements can be achieved by using t_{99} . This is particularly useful when the purity is considered as one of the critical quality attributes alongside mean crystal size.

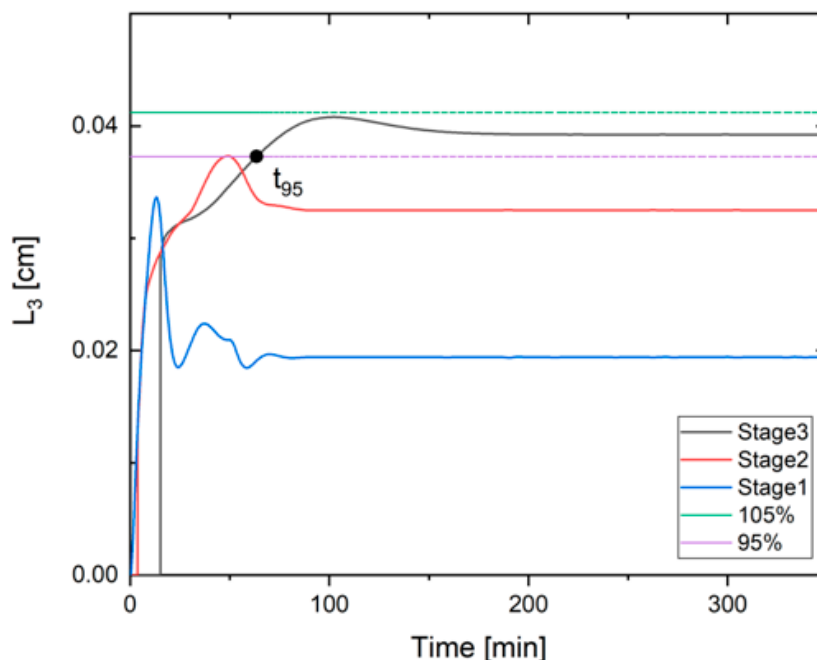


Figure 3. Dynamic profiles of the mean crystal size at different crystallization stages during startup.

4. Conclusions

A systematic and rigorous model-based optimization approach was implemented to the combined cooling and antisolvent crystallization of ASA in continuous MSMR cascade crystallizers. The steady state optimization approach, based on the attainable regions, made it possible to design a cascade of three MSMR crystallizers. In addition, it was possible to identify the optimal temperature, antisolvent flowrate and residence time for each MSMR.

The minimization of startup is a major challenge in continuous pharmaceutical manufacturing due to the anticipated short operating windows. In order to minimize the startup time of the cascade of MSMR crystallizers, which in turn maximizes the efficiency by reducing waste and increasing on-specification products, several dynamic optimization strategies were implemented. More realistic scenarios were considered by starting from empty MSMR vessels. To address the dynamic optimization problem, several decision/control variables and discretization rules were adopted to enhance the available degrees of freedom and achieve a more effective optimization. The optimal dynamic profile of cooling temperature, antisolvent flowrate, and seed addition were identified and compared. Only the optimal profile of antisolvent flowrates is presented here for the sake of brevity. It was shown that the startup optimization improves the startup time by 26.77% and 31.3%, which represents a significant gain in terms of production and waste minimization.

Reference

1. Mascia, S.; Heider, P.L.; Zhang, H.; Lakerveld, R.; Benyahia, B.; Barton, P.I.; Braatz, R.D.; Cooney, C.L.; Evans, J.M.B.; Jamison, T.F.; et al. End-to-End Continuous Manufacturing of Pharmaceuticals: Integrated Synthesis, Purification, and Final Dosage Formation. *Angew. Chem. Int. Ed.* **2013**, *52*, 12359–12363.
2. Benyahia, B.; Lakerveld, R.; Barton, P.I. A Plant-Wide Dynamic Model of a Continuous Pharmaceutical Process. *Ind. Eng. Chem. Res.* **2012**, *51*, 15393–15412.

3. Fysikopoulos, D.; Benyahia, B.; Borsos, A.; Nagy, Z.K.; Rielly, C.D. A Framework for Model Reliability and Estimability Analysis of Crystallization Processes with Multi-Impurity Multi-Dimensional Population Balance Models. *Comput. Chem. Eng.* **2019**, *122*, 275–292.
4. Nagy, Z.K.; Fujiwara, M.; Braatz, R.D. Modelling and Control of Combined Cooling and Antisolvent Crystallization Processes. *J. Process Control* **2008**, *18*, 856–864.
5. Lakerveld, R.; Benyahia, B.; Heider, P.L.; Zhang, H.; Wolfe, A.; Testa, C.J.; Ogden, S.; Hersey, D.R.; Mascia, S.; Evans, J.M.B.; et al. The Application of an Automated Control Strategy for an Integrated Continuous Pharmaceutical Pilot Plant. *Org. Process Res. Dev.* **2015**, *19*, 1088–1100.
6. Benyahia, B. *Applications of a Plant-Wide Dynamic Model of an Integrated Continuous Pharmaceutical Plant: Design of the Recycle in the Case of Multiple Impurities*, 1st ed.; Elsevier: Amsterdam, The Netherlands, 2018; Volume 41.
7. Su, Q.; Benyahia, B.; Nagy, Z.K.; Rielly, C.D. Mathematical Modeling, Design, and Optimization of a Multisegment Multiaddition Plug-Flow Crystallizer for Antisolvent Crystallizations. *Org. Process Res. Dev.* **2015**, *19*, 1859–1870.
8. Yang, Y.; Nagy, Z.K. Combined Cooling and Antisolvent Crystallization in Continuous Mixed Suspension, Mixed Product Removal Cascade Crystallizers: Steady-State and Startup Optimization. *Ind. Eng. Chem. Res.* **2015**, *54*, 5673–5682.
9. Lindenberg, C.; Krättli, M.; Cornel, J.; Mazzotti, M.; Brozio, J. Design and Optimization of a Combined Cooling/Antisolvent Crystallization Process. *Cryst. Growth Des.* **2008**, *9*, 1124–1136.
10. Barik, K.; Prusti, P.; Mohapatra, S.S. Single- and Multi-Objective Optimisation for a Combined Cooling and Antisolvent Semi-Batch Crystallisation Process with an ACADO Toolkit. *Indian Chem. Eng.* **2020**, *62*, 287–300.
11. Parekh, R.; Benyahia, B.; Rielly, C.D. *A Global State Feedback Linearization and Decoupling MPC of a MIMO Continuous MSMPR Cooling Crystallization Process*; Elsevier: Amsterdam, The Netherlands, 2018; Volume 43.
12. Benyahia, B.; Latifi, M.A.; Fonteix, C.; Pla, F. Multicriteria dynamic optimization of an emulsion copolymerization reactor. *Comput. Chem. Eng.* **2012**, *35*, 2886–2895.

Publisher's Note: MDPI stays neutral with regard to jurisdictional claims in published maps and institutional affiliations.



© 2020 by the authors. Licensee MDPI, Basel, Switzerland. This article is an open access article distributed under the terms and conditions of the Creative Commons Attribution (CC BY) license (<http://creativecommons.org/licenses/by/4.0/>).